33

Breaking of Super-Critically Incident Internal Waves at a Sloping Bed

I. P. D. De Silva, J. Imberger and G. N. Ivey

Abstract

A laboratory experiment was carried out to investigate the mixing on a sloping bed caused by a localised ray of internal waves breaking with super-critical frequencies. Previous work has shown that for near critical waves the turbulent boundary layer was confined to a thin region just above the bed. As a result, relatively small overturning turbulent lengthscales were observed. On the other hand, larger turbulent lengthscales and more mixing occurred at moderately super-critical waves, consistent with some earlier laboratory results. Calculation of the energy budget of the incident and reflected wave rays showed the vertical diffusivities as high as 10^{-4} m^2 s^{-1} observed in field studies could be realised by the internal wave breaking process at the boundaries.

Introduction

Field studies on natural lakes show significant vertical fluxes in the benthic boundary layer generated by the breaking of internal waves which can be responsible for much of the vertical transport of mass and momentum in the hypolimnion (Saggio and Imberger, 1995; Lemckert and Imberger, 1998). The lack of measurements in the abyssal seas and the mismatch in vertical diffusivities betweem those required for the abyssal budget and those frequently measured directly in the open ocean (e.g. Gregg, 1998), suggest that most of the mass flux may take place near the ocean boundaries. Armi (1978) first suggested that the turbulence was generated by mesoscale current drag against the sea-floor. This suggestion was shown to be unlikely by Garrett (1979 as the typical ocean stratifications and the conversion efficiency could not permit the high mixing rates suggested by Armi (1978) due to mean flows. Thus, internal wave breaking at the boundaries seems to be the most likely cause of the observed net vertical fluxes.

Armi (1978) suggested that the effective vertical diffusivity of a stratified basin may be written as $K = K_b A_r$, where K_b is the vertical diffusivity in the boundary layer, A_r is the ratio of horizontal area occupied by the boundary layer to the horizontal area of the basin. However, Garrett (1979) and Ivey (1987) pointed out that this required the bottom boundary layer to be stratified like the interior. For a basin of diameter L, with a boundary layer of thickness δ and slope angle β, the area ratio becomes $A_r \sim \delta/(L \sin \beta)$. Using

Physical Processes in Lakes and Oceans
Coastal and Estuarine Studies Volume 54, Pages 475-484
Copyright 1998 by the American Geophysical Union

typical values for the ocean of $\beta \sim 4^{\circ}$ (Bell, 1975), $\delta \sim 50$ m, $L \sim 4 \times 10^6$ m (Armi, 1978) we find that in the ocean $A_r \sim 1.8 \times 10^{-4}$; for lakes, $\beta \sim 10^{o}$, $\delta \sim 2$ m, $L \sim 10 \times 10^3$ m, and thus $A_r \sim 1 \times 10^{-3}$. Thus, assuming comparable values of K_b in the ocean and in lakes, the boundary mixing process has a bigger impact in lakes than in oceans.

The no flux condition at the solid boundary requires the frequency of the reflected wave to be the same as the incident wave. The wave frequency ω of a small amplitude internal wave ray is related to the stable buoyancy frequency N by $\omega = N \sin \alpha$, where α is the inclination of the wave group velocity vector to the horizontal, and N is the background buoyancy frequency, defined by

$$N^2 = -\frac{g}{\rho_r}\frac{d\rho}{dz} \tag{1}$$

Here ρ is the density, ρ_r is a reference density, g is the acceleration due to gravity and z is the vertical coordinate. Thus both the incident and reflected wave rays make equal angles to the vertical. Phillips (1977), Eriksen (1982, 1985) and Imberger (1994) have shown that an increase in energy density of the reflected ray results upon reflection. For the critical case where the group velocity of the reflected wave becomes parallel to the slope ($\alpha = \beta$), the reflected wave amplitude increases without bound, indicating a singularity in the linear theory. Eriksen (1982, 1998) illustrated this condition in the field, where an intensification of horizontal kinetic energy was observed. In what follows, for a given incident wave field of frequency ω, we define the parameter,

$$\gamma = \omega/\omega_C, \tag{2}$$

where $\omega_C = N \sin \beta$ is the critical frequency.

At the boundary, a fraction of the energy of the incident wave is radiated away as a reflected ray and a part of the energy is lost to dissipation. The difference is converted into a buoyancy flux which accounts for the observed vertical transport of mass. The ratio of the amount of energy carried away by the reflected wave ray to that in the incident wave is defined as the reflection coefficient C_r. The exact dependence of C_r on the incident wave parameters such as the wave steepness and the geometry γ is not known. However, the numerical simulations of Javam et al. (1997a) showed that for a wide range of γ, C_r is approximately given by

$$C_r = -0.122\,\gamma^2 + 0.855\,\gamma - 0.613. \tag{3}$$

Another parameter which is not accurately known is the mixing efficiency R_f, defined as the ratio of the increase in potential energy due to mixing divided by the incident energy flux. Ivey and Nokes (1989, 1990) demonstrated that R_f is strongly dependent on γ. Further, their experiments showed that $R_f \approx 0$ for $\gamma < 0.7$, $R_f \approx 0.2$ for $\gamma \approx 1$ (cf. Taylor 1993) and a maximum of R_f was observed around $\gamma \approx 1.2$. Numerical simulations of Slinn and Riley (1996) found that for $\gamma \approx 1$, $R_f \approx 0.35$ and $C_r \approx 0.10$.

The non-linear analysis of Thorpe (1987), showed that the interaction of incident and reflected waves can produce higher modes with frequencies larger than the ambient buoyancy frequency, thus generating evanescent modes. The same feature has also been observed for two intersecting wave rays in the numerical simulations of Javam et al. (1997b) and laboratory experiments of Teoh et al. (1997). These studies showed that wave reflection at a boundary possessed many similarities to the non-linear interaction of two intersecting wave beams.

Experiments

The experiments were conducted in a tank of dimensions 590 cm × 54 cm × 60 cm. At one end of the tank a 2 cm thick plexiglass sheet was used as the sloping bed. This sheet was pivoted about a horizontal axis 12 cm above the tank bottom, so that the slope angle could be varied. The internal wave rays were generated using a triangular shaped folding paddle, adapted from the original design of McEwan (1973). The paddle was made up of eight 5 cm long by 53 cm wide, hinged blades that spanned the width of the tank (for details see Teoh et al., 1997 and De Silva et al., 1997). The internal wave ray tube radiating from the paddle was approximately 1.5 wavelengths wide (Figure 1) while the wavelength was approximately 20 cm. The paddle was mechanically linked to an eccentric wheel, driven by a heavy-duty, adjustable D.C. motor. By varying the eccentricity of the wheel, the paddle amplitude could be varied. In this study, we report a series of runs with a paddle amplitude of 3.1 cm.

The tank was filled with a linearly stratified salt solution using a standard two-tank technique and the depth of the water column was approximately 48 cm. The temperature of the fluid column was measured using a fast response FP07 thermistor while the salinity was measured using two sensors: a fast response micro-scale conductivity probe for turbulence measurements and a suction probe for mean conductivity measurements. Vertical casts of temperature and conductivity were obtained by traversing the sensors through the fluid column at a set speed of 10 cm s^{-1} using a computer controlled linear translator. Both the direct and differentiated output from each sensor was recorded at a sampling frequency of 100 Hz through a 16-bit analog-digital converter.

The paddle oscillating frequency was chosen according to the stratification and α. The experiments were started by commencing the paddle oscillations from a rest state and the oscillations were maintained steadily throughout the duration of the experiment.

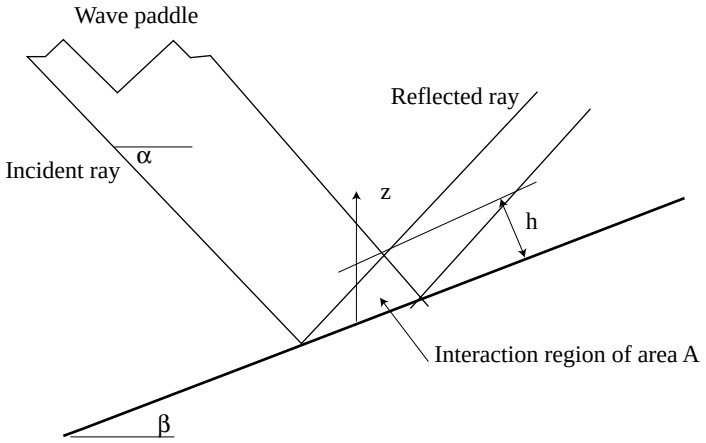

Figure 1. Schematic of internal wave reflection.

Results

For forward reflecting waves ($\gamma > 1$), the non-dimensional height normal to the bed h/λ, and the non-dimensional area A/λ^2, of the incident and reflected wave interaction region, can be shown to be

$$\frac{h}{\lambda} = \frac{\sin(\alpha - \beta)}{2\cos\alpha}, \tag{4a}$$

$$\frac{A}{\lambda^2} = \frac{\tan\alpha \sin(\alpha - \beta)}{4\sin(\alpha + \beta)}, \tag{4b}$$

by geometric linear ray theory, where A is the area of the interaction region in the vertical plane and λ is the horizontal wavelength of the incident wave field (Figure 1). Thus, for a given α the depth of the interaction region increases from zero at the critical condition to a maximum of $(\lambda \tan \alpha)/2$ when $\beta = 0$. Figure 2 shows how h/λ and A/λ^2 increase with increasing γ for a given incident wave field. In this example $\alpha = 56^\circ$, the condition relevant to the runs described later in the paper. Both h and A initially increase rapidly as the incident wave becomes progressively super-critical, asymptoting to constant values for large γ. For example, from $\gamma = 1.5$ to $\gamma = 3$ the increase in h and A is approximately two-fold, whereas from $\gamma = 3$ to $\gamma = 6$ the increase is relatively small.

Flow visualisation images of Ivey et al. (1995) and De Silva et al. (1997) indicated that near critical conditions the motion was dominated by a thin, sheared, parallel flow just above the bed and superimposed on the background ambient wave field. This observation is consistent with the result in (4), that the interaction area in such situations becomes rather small. On the other hand, at super-critical frequencies the visualisation images

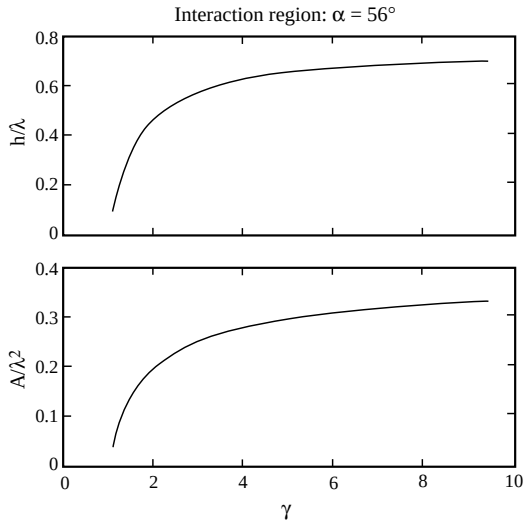

Figure 2. The variation of (a) the non-dimensionless extent of the interaction area (h/λ) and (b) the non-dimensionless area (A/λ^2) of the interaction region with γ.

showed that this strong shearing flow extended farther away from the bed. Work by Thorpe (1987) and Javam et al. (1997a) have shown that the boundary reflection process may be considered as the interaction of waves which comprise the incident, the reflected and the higher harmonics in the interaction region. According to Teoh et al. (1997), such interactions produce waves at frequencies higher than the ambient buoyancy frequency and these evanescent wave modes can lead to instabilities by absorbing energy from the primary waves through a non-linear, non-resonant interaction mechanism.

Turbulent Quantities

The turbulent quantities described here were obtained from the vertical casts of the temperature, density and their respective gradient profiles. The estimation of turbulent dissipation was central to the analysis, hence it is described first.

The estimation of turbulent kinetic energy dissipation rate ε by fitting the Batchelor spectra to the spectra of the measured temperature gradient signal using ε as a free parameter has been common in field studies (Dillon and Caldwell, 1980; Imberger and Boashash, 1986; Luketina, 1987) and in laboratory studies (Teoh, 1997; De Silva et al., 1997). The portion of the wavenumber spectra from the maximum down through the roll-off region was used in a curve-fitting procedure (e.g. Luketina, 1987). A typical measured temperature gradient spectra and the fitted spectra are shown in Figure 3 where the number of points used for the spectra was 128. With the sensor travelling at speeds of 10 cm s^{-1} and a sampling rate of 100 Hz, the Nyquist wavenumber cut-off was 500 cpm.

An overturning lengthscale characterising the turbulence was estimated using the vertical casts from the density profiles. This process involved two stages. Firstly, the recorded profile $\rho(z)$ with overturns was monotonised to obtain the statically stable density profile $\rho_O(z)$, which was associated with the minimum potential energy. The vertical distances l_d each fluid parcel has to be displaced to achieve this monotonised profile are known as the Thorpe displacements (Thorpe, 1977). Using the values of l_d, a single lengthscale l_c characterising the energy containing eddies in a single turbulent patch was calculated, as outlined in Imberger and Boashash (1986). This centralised lengthscale l_c,

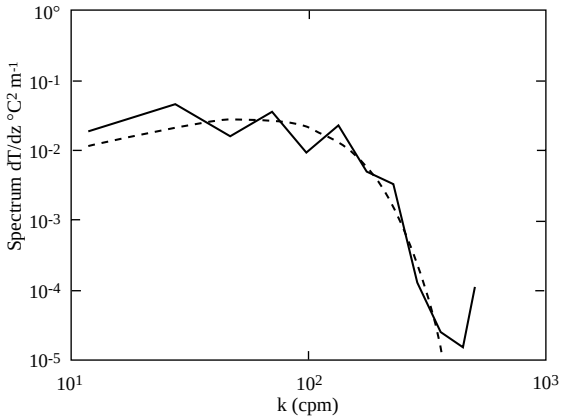

Figure 3. The wavenumber spectra of the temperature gradient signal and the fitted Batchelor spectra. The experimental conditions are, a = 3.1 cm, N = 0.615 rad/s, α = 32.5° and β = 10.2°.

is calculated by displacing the individual displacement scales l_d to the centre of the event by one-half of the l_d values themselves and taking the r.m.s of all values.

Based on the turbulent lengthscale l_c and dissipation rate ε, a turbulent velocity scale may be defined as $u = (\varepsilon l_c)^{1/3}$. The non-dimensional numbers associated with stratified turbulence may then conveniently be defined as (Ivey and Imberger, 1991; Imberger and Ivey, 1991; Imberger, 1994) as the turbulent Reynolds number, $Re_t = ul_c/\nu$, the strain Froude number, $Fr_\gamma = (\varepsilon/\nu N^2)^{1/2}$ and the turbulent Grashof number, $Gr_t = N^2 l_c^4/\nu^2$. These numbers can be successfully used to infer the mixing efficiency in stratified turbulence as shown by Imberger and Ivey (1991), for example. The above non dimensional numbers can also be interpreted as lengthscale ratios formed from l_c, the Ozmidov scale $l_O = (\varepsilon/N^3)^{1/2}$, where the buoyancy affects the motion, and the Kolmogorov scale $l_K = (\nu^3/\varepsilon)^{1/4}$, where the viscosity suppresses the motion, as $Fr_\gamma = (l_O/l_K)^{2/3}$ and $Re_t = (l_c/l_K)^{4/3}$. In general, a buoyancy flux occurs when there exists a range of overturning scales l_c between l_O and l_K. Gr_t describes the ratio of the buoyancy force which tries to bring a displaced fluid particle back to its neutral buoyancy level to the restraining forces due to viscous effects. Alternatively, it can also be related to the ratio of two timescales, the buoyancy timescale $t_b \sim N^{-1}$ and the viscous diffusion timescale $t_\nu \sim l_c^2/\nu$; thus $t_b/t_\nu \sim [l_c/(\nu/N)^{1/2}]^{-2} \sim Gr_t^{-1/2}$. When $t_b < t_\nu$, or $Gr_t > 1$, the buoyancy forces dominate over the viscous forces (Imberger, 1994).

Thorpe (1987) showed the importance of incident wave steepness as a parameter in defining the existence of statically unstable regions in the flow domain. His results indicated that for given β, the incident wave steepness at which a statically unstable region occurs increases as γ increases. The present incident wave parameters (the steepness, α, β) are, however, beyond the range covered in Thorpe (1987), and no direct comparison can be made. In this paper, we present a series of experiments keeping the incident wave steepness the same but varying slope angles to investigate the dependence of turbulent quantities on γ.

Results of De Silva et al. (1997) and Taylor (1993) indicated that there is a strong variability of turbulent properties within a wave cycle. This variability can be as high as two orders of magnitude (see Figure 12 of Taylor, 1993, for example). However, a useful overview may be obtained from the cycle averaged quantities, which are shown in Figure 4. As pointed out before, near critical conditions with $\gamma \approx 1$ the dominant feature of the interaction region was a highly sheared narrow parallel flow just above the bed as expected from (4). The thickness of this region was small so that relatively small displacement scales l_c were observed (practical difficulties associated in traversing the probe very close to the slope may have also contributed to the decrease of levels of the lengthscales in this case). The cause of the decrease in Fr_t for highly supercritical waves ($\gamma \approx 3$) is not clear, but it could have been due to the decrease in energy density available for the fluid to generate overturns, associated with the rapid increase in the interaction area (according to Figure 2b, the increase in area is about a factor three from $\gamma \approx 1.5$). The fact that $Gr_t < 1$ near $\gamma \approx 1$ clearly shows that the scales of the motion are strongly affected by the viscosity, whereas in the range $2 < \gamma < 3$, they are not. These non-dimensional numbers are cycle averaged, and one should not discount the fact that there is a strong variation in the turbulent quantities over a wave cycle. The point to note is that there is a certain portion of the wave cycle during which Fr_γ is high and it is this time period during which mixing likely takes place. More mixing seem to take place in the range $2 < \gamma < 3$ than it does for near critical waves.

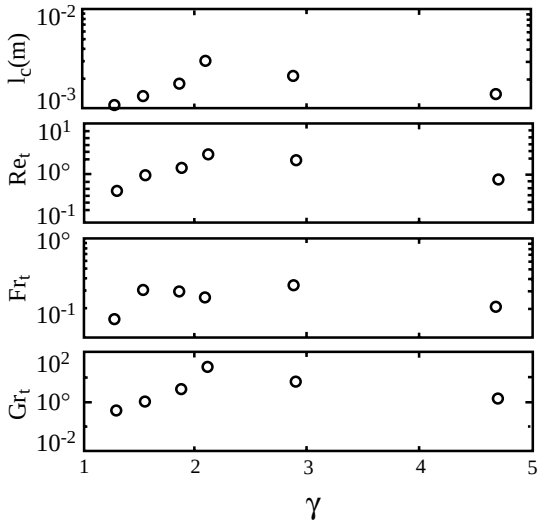

Figure 4. Variation of cycle averaged l_c, Re_t, Fr_t and Gr_t with the parameter γ. The first three panels are extracted from De Silva et al. (1997). The experimental conditions are a = 3.1 cm, N = 0.615 rad/s and $\alpha = 56°$.

Effective Vertical Diffusivity

It is of interest to oceanographers and limnologists to quantify the effective vertical exchange coefficients for mass and momentum for the turbulence generated by the internal wave breaking process. Relatively high diffusivities, for example of the order of 10^{-4} m^2 s^{-1} compared to the typical interior values of 10^{-5} m^2 s^{-1}, have been reported near the boundaries (Ledwell and Hickey, 1995; Lemckert and Imberger, 1998). Due to the horizontal pressure gradient between the locally mixed region at the boundary and the ambient stratification, boundary mixed fluid can intrude horizontally into the fluid interior along isopycnals. For the present configuration, De Silva et al. (1997) showed that the intrusion follows a viscous-buoyancy balance and spreads into the main fluid body with a length $l \propto t^{5/6}$ power law, as schematically shown in Figure 5. In natural water bodies, these intrusions carry nutrient rich benthic water into the interior enhancing the plankton growth.

The amount of vertical mixing generated by the breaking waves depends on the nature of the incident wave field, the strength of the stratification and the bottom geometry. Here we present a simple energy argument to estimate an effective turbulent vertical diffusivity for the wave breaking process. Consider an incident wave field of amplitude a and frequency ω, approaching a sloping bed; the wave energy per unit mass is of the order a^2N^2, so that the amount of wave energy available at the bed per unit mass per unit time is of the order $a^2N^2\omega$. For super-critical waves part of this energy is reflected in the form of a reflected wave at the bed. Denoting the ratio of the amount of energy taken away by the reflected wave to that incident at the bed by C_r, the amount of energy trapped in the interaction region would be $a^2N^2\omega(1 - C_r)$. Following Ivey and Imberger (1991), the mixing efficiency R_f is defined as the ratio of the buoyancy flux to the amount of energy

available for mixing. Thus for the internal wave breaking in the interaction region, the buoyancy flux b can be written as,

$$b \sim a^2N^2\omega(1 - C_r)R_f. \quad (5)$$

Now it is possible to determine the local, effective vertical exchange coefficient for mass as $K_{eff} = b/N^2$, thus,

$$K_{eff} \sim a^2\omega(1 - C_r)R_f. \quad (6)$$

The difficulty in using the above equation lies in the fact that the exact dependence of R_f and C_r are not known. Equation (6) for K_{eff} may be rewritten in the form,

$$K_{eff} \sim a^2\gamma(1 - C_r)R_f N\sin\beta. \quad (7)$$

The only available information on the R_f dependence on γ is due to the work of Ivey and Nokes (1990) (see also Ivey et al, 1995). Taking a conservative value of $R_f = 0.2$, C_r from (3) and using the typical values of for a lake, a = 2 m, N = 10-3 rad/s, $\beta = 10°$ and $\gamma \approx 2$, we get $C_r \approx 0.6$, and $K_{eff} \approx$ 10-4 $m^2\ s^{-1}$, which agrees well with the high diffusivity levels observed near boundaries in some field experiments (Lemckert and Imberger, 1998; Wüest and Gloor, 1998).

Conclusions

We have described an experimental study of the breaking of a ray of internal waves on a sloping bed at varying bed angles. Previous work (De Silva et al., 1997) showed that near critical conditions the flow was confined to a thin region in the vicinity of the slope superimposed on the ambient wave motion. As a result, relatively small turbulent lengthscales, and hence small turbulent Reynolds numbers, were observed. The mechanism for off slope instabilities seems to be due to the interaction of incident and reflected waves (Thorpe, 1987; Teoh et al., 1997; Javam et al., 1997a,b); this was absent at critical conditions. Within the range of bed angles considered, the largest lengthscales occurred in the range $1.5 < \gamma < 2$. For highly supercritical waves ($\gamma > 3$), the overturning length-scales again decreased. Simple energy budgets in the interaction region reveal a possibility of realising enhanced vertical diffusivity for the wave breaking process.

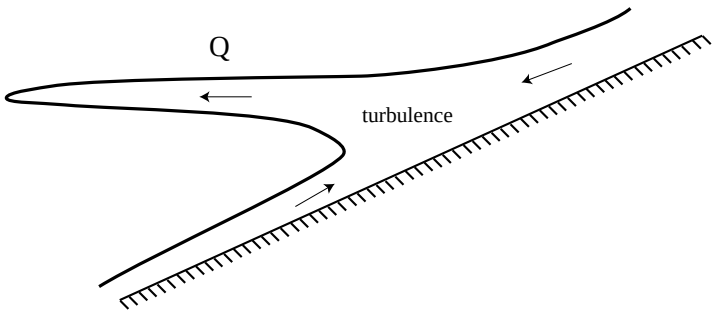

Figure 5. Schematic of the intrusion flow generated by the internal wave breaking process.

However, the comparison of field experiments to the present laboratory experiments should be done with caution, as there is a strong variability in the turbulence field within a wave period.

Acknowledgments. This work was supported by the Australian Research Council and the Centre for Environmental Fluid Dynamics program. Most of the work presented here was presented at the 1995 IUTAM symposium in Broome, Australia. The authors gratefully acknowledge constructive comments by the participants of the conference. One of us, IPDeS would like to thank Joe Fernando for his continued encouragement. This paper is Centre for Water Research reference ED-1004-PDS.

References

Armi, L. Some evidence for boundary mixing in the deep ocean. *J. Geophys. Res., 83*, 1971-1979, 1978.

De Silva, I. P. D., J. Imberger, and G. N. Ivey. Localised mixing due to a breaking internal wave ray at a sloping bed. *J. Fluid Mech*., 350, 1-27, 1997.

Dillon, T. M. and D. R. Caldwell, The Batchelor spectrum and dissipation in the upper ocean. *J. Geophys. Res., 85*, 1910-1916, 1980.

Eriksen, C. C. Observations of internal wave reflection off sloping bottoms. *J. Geophys. Res., 87*, 525-538, 1982.

Eriksen, C. C. Implications of ocean bottom reflection for internal wave spectra and mixing. *J. Phys. Oceanogr., 15*, 1145-1156, 1985.

Eriksen, C. C. Waves, mixing, and transports over sloping boundaries, in *Physical Processes in Lakes and Oceans*, edited by J. Imberger, pp 402-424 this volume, 1998.

Garrett, C. Comments on "Some evidence for boundary mixing in the deep ocean." by L. Armi. *J. Geophys. Res., 84*, 5095, 1979.

Gregg, M. C. Estimation and geography of diapycnal mixing in the stratified ocean, in *Physical Processes in Lakes and Oceans*, edited by J. Imberger, pp 294-326, this volume, 1998.

Imberger, J. Transport processes in lakes: A review, in *Limnology Now: A Paradigm of Planetary Problems*, edited by R. Margalef, pp 99-193, Elsevier, 1994.

Imberger, J. and B. Boashash, Application of the Wigner-Ville distribution to temperature gradient microstructure: A new technique to study small-scale turbulence. *J. Phys. Oceanogr., 16*, 1997-2012, 1986.

Imberger, J. and G. N. Ivey, On the nature of turbulence in a stratified fluid. Part II: Application to lakes. *J. Phys. Oceanogr., 21*, 659-680, 1991.

Ivey, G. N., The role of boundary mixing in the deep ocean. *J. Geophys. Res., 92*, 11,873-11,878, 1987.

Ivey, G. N. and R. I. Nokes, Vertical mixing due to the breaking of critical internal waves on sloping boundaries. *J. Fluid Mech., 204*, 479-500, 1989.

Ivey, G. N. and R. I. Nokes, Mixing driven by the breaking of internal waves against sloping boundaries. *Proc. Intl. Conf. on Physical Modelling of Transport and Dispersion*, MIT, Boston, 11A3-11A8, 1990.

Ivey, G. N. and J. Imberger, On the nature of turbulence in a stratified fluid. Part I: The energetics of mixing. *J. Phys. Oceanogr., 21*, 650-658, 1991.

Ivey, G. N., I. P. D. De Silva, and J. Imberger, Internal waves, bottom slopes and boundary mixing. *Aha Hulikoa winter workshop*. Honolulu, Hawaii, 199-205, 1995.

Javam, A., J. Imberger, and S. Armfield, Numerical study of internal wave overturning on a sloping boundary. Revised and resubmitted to *J. Fluid Mech*., 1997a.

Javam, A., J. Imberger, and S. Armfield, Numerical study of internal wave-wave interactions. Revised and resubmitted to *J. Fluid Mech*., 1997b.

Ledwell, J. R. and B. M. Hickey, Evidence for enhanced boundary mixing in the Santa Monica basin. *J. Geophys. Res., 100*, 665-679, 1995.

Lemckert, C. and J. Imberger, Turbulent boundary layer mixing events in fresh water lakes, in *Physical Processes in Lakes and Oceans*, edited by J. Imberger, pp 503-516, AGU, this volume, 1998.

Luketina, D. A. Frontogenesis of freshwater overflow. PhD dissertation. University of Western Australia, 1987.

McEwan, A. D. Interactions between internal gravity waves and their traumatic effect on a continuous stratification. *Boundary-Layer Met., 5*, 159-175, 1973.

Phillips, O. M., Dynamics of the upper ocean. Cambridge University Press., 1977.
Saggio, A. and J. Imberger, Internal wave climatology in lake Biwa. In Preparation, 1995.
Slinn, D. N. and J. J. Riley, Turbulent mixing in the oceanic boundary layer due to internal wave reflection from sloping terrain. *Dyn. Atmos. Oceans, 23*, 51-62, 1996.
Taylor, J. R., Turbulence and mixing in the boundary layer generated by shoaling internal waves. *Dyn. Atmos. Oceans, 19*, 233-258, 1993.
Teoh, S. G., G. N. Ivey, and J. Imberger, Laboratory study of the interactions between two internal waves. *J. Fluid Mech., 336*: 91-122, 1997.
Thorpe, S. A., Turbulence and mixing in a Scottish loch. *Phil. Trans. Roy. Soc. London, A, 286*, 125-181, 1977.
Thorpe, S. A., On the reflection of a train of finite-amplitude internal waves from a uniform slope. *J. Fluid Mech., 178*, 279-302, 1987.
Wüest, A. and M. Gloor, Bottom boundary mixing in lakes: The role of the near-sediment density stratification, in *Physical Processes in Lakes and Oceans*, edited by J. Imberger, pp 485-502, AGU, this volume, 1998.